

Experimental Research on Thermal-mechanical Properties of Shape Memory Alloys

Tiger Hu Sun*, Zhihang Jia, Junyu Ge

Faculty of Civil Engineering and Mechanics, Jiangsu University, Zhenjiang, Jiangsu, China

Abstract More attentions have been paid to Shape Memory Alloys (SMAs), which is a kind of excellent functional materials. In this work, a special device was designed for the test of the mechanical behaviors of SMAs, which includes three modules, separately: tension module, torsion module and temperature-controlled cabinet. In work, it will be assembled on Mechanical Testing & Simulation MTS-858. The typical thermal-mechanical properties of SMAs were investigated systematically, involving the responses and the heating-induced strain recovery under proportional and nonproportional tensile-torsional loadings at various temperatures. The results show that the response of the SMAs under pure tension is quite different from that under pure torsion. In the case of constrained heating-induced recovery stress, it is found that the recovery resistance increases with the increase of pre-deformation. Recovery stress at various recovery strains and the thermal-mechanical properties of the SMAs subjected to cyclic straining were investigated.

Keywords Shape Memory Alloys, Special Testing Device, Samples, Experiment

1. Introduction

Shape memory alloys (SMAs) are composed of austenite and martensite, the forward and reverse thermo-elastic martensitic transformation determines the amazing properties of SMAs [1-3]. When a SMA is cooled down to below some critical temperature, it will mainly be composed of martensite and can be manipulated easily in a very large strain range [4-6]. When it is heated to above some critical temperature, it will change back to the austenite phase, the previous in-elastic deformation will be recovered and it will resume the shape it normally has at the higher temperature, this is shape memory effect (SME). At higher temperature, applied stress may cause martensitic transformation and a SMA may deform in-elastically, but the in-elastic deformation may be recovered as the applied stress is removed, which is referred to as pseudo-elasticity (PE) [7]. Because of these particular properties, SMAs have been widely used in various fields [8-12].

Compared with other SMAs, $\text{Ni}_{47}\text{Ti}_{44}\text{Nb}_9$ has a greater transformation hysteretic loop and a high strain recovery rate [13-16]. Zhao and Zhang found that in SMA $\text{Ni}_{47}\text{Ti}_{44}\text{Nb}_9$ there exists a characteristic deformation temperature M_s+30 °C and critical strain range 16%, at which deformation

can effectively increase inverse transformation temperature and transformation hysteretic loop while maintaining a high strain recovery rate [17]. Experimental studies about SMA $\text{Ni}_{47}\text{Ti}_{44}\text{Nb}_9$ mainly focus on the uniaxial tensile properties and corresponding heat recovery characteristics, but the works for the response characteristics under complex and pure torsional paths are seldom. In this work, a special device for the test of the mechanical behaviors of SMAs was designed, which includes three modules, separately, tension module, torsion module and temperature-controlled cabinet. Aiming to SMA specimen $\text{Ni}_{47}\text{Ti}_{44}\text{Nb}_9$, the series of experimental were investigated, including: experimental methods, combined tension-torsion loading experiments, cooling experiments, low temperature experiments and heating experiments.

2. Samples of $\text{Ni}_{47}\text{Ti}_{44}\text{Nb}_9$ Alloys

Samples of $\text{Ni}_{47}\text{Ti}_{44}\text{Nb}_9$ alloys manufactured by Research Institute for Nonferrous Metals located in Beijing are used in the test, and the composition provided by the manufacturer of the materials are shown in Table.1.

Table 1. Chemical compositions of testing material Wt%

Ti	Nb	C	O	Ni
36.5	14.5	<0.01	<0.04	remaining

Thin-walled cylindrical specimens are adopted in the test, including a testing part located in the middle of sample, and a connection part on its both ends. Dimensions of specimens are shown in Fig.1. It can be seen from that, the diameter of

* Corresponding author:

ts420@ujs.edu.cn (Tiger Hu Sun)

Published online at <http://journal.sapub.org/materials>

Copyright © 2019 The Author(s). Published by Scientific & Academic Publishing

This work is licensed under the Creative Commons Attribution International

License (CC BY). <http://creativecommons.org/licenses/by/4.0/>

connection part is bigger than that of testing part, and an outer screw thread is provided in the surface of the former. In addition, each connection part is processed with two parallel step surfaces marked 3 as shown in Fig.1, which is parallel to the axis of sample.

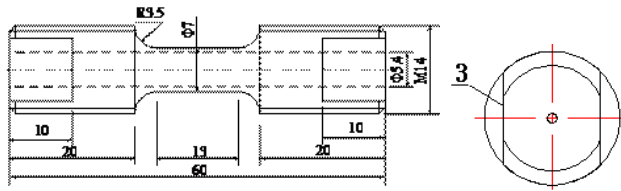


Figure 1. Dimensions of specimen

3. Experimental Testing Device

The testing device is shown in Fig.2. The fixture is placed in the temperature-controlled cabinet, assemble this device on the MTS-858, the uniaxial tension, pure shearing, proportional loading and nonproportional loading testing can be completed.



Figure 2. The testing device

3.1. Specimen Fixture

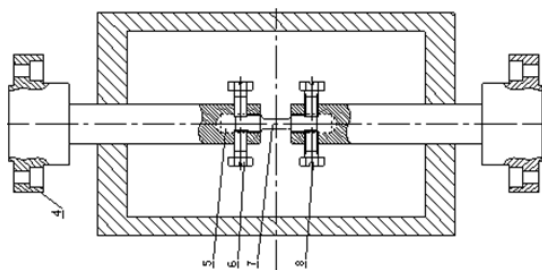


Figure 3. Schematic diagram of the testing device

The shape of fixture unit is cylindrical, one end with a coaxial flange marked as 4 in Fig.3, and the other end with a coaxial inner bore marked as 5 in Fig.3. The inner bore is processed with internal thread, in use, it will be matched with external thread in surface of the test specimen. In addition, there are two thread-holes located at opposite sides of cylindrical surface of fixture. The two bolts marked as 6 in Fig.3 are connected to the fixture by matching with them, and continue turn bolts, until its inside end firmly hold against parallel step surfaces marked as 3 in Fig.1, the later is

perpendicular to the axis of the former. By this method, specimen can be fixed well on fixture, and its rotation can be prevented during test.

3.2. Temperature-controlled Cabinet

Temperature-controlled cabinet comprises temperature control box and the rails, one end of the later extending to the above of the worktable, and the former is fitted on the rail by roller, so it can be moved along the track. The top and bottom of the temperature control box are provided with a through hole, two clamps can pass through them, and respectively connected with the lower and the upper flanges of MTS-858. Making use of the temperature control box, the requirements for temperature change can be satisfied in test.

3.3. Assemble

In test, first mobilizable temperature control box puts the top of worktable, then the fixture is bolted with the lower and the upper flange of MTS-858, and the test piece is fitted to fixture inside the temperature control box. When all of these mentioned above finish, together with tension-torsion testing system of MTS-858, then tension-torsion testing of SMAs can be completed according to the set program.

When mounting the specimen, the connection part of the sample is screwed into the hole of the fixture, then two bolts on opposite sides of fixture is crewed tightly against the step surface in the connecting portion of the specimen, which can prevent rotation of the specimen very well and satisfy the specimen mounting and fixing. The testing machine and temperature control chamber are shown in Fig.4.

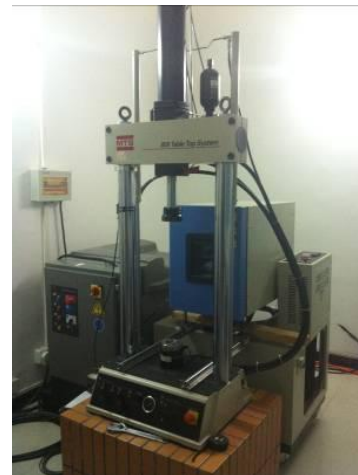


Figure 4. The testing machine and temperature control chamber

The tests are conducted on Electro-hydraulic servo low cycle fatigue tension-torsion testing machine MTS-858. The ranges of axial load and torque loads are $\pm 15\text{kN}$ and $\pm 100\text{N}\cdot\text{m}$. Test temperature is controlled by temperature control chamber, and its change range is $-70\text{ }^{\circ}\text{C}$ to $150\text{ }^{\circ}\text{C}$. The fluctuation of temperature during operation is less than $\pm 0.5\text{ }^{\circ}\text{C}$, and the temperature uniformity is $\pm 2\text{ }^{\circ}\text{C}$. During the test, axial loading is applied by displacement, and torsional loading is controlled by torsion angle. The test is quasi-static

loading, loading velocity is designed as $1.3 \times 10^{-4} \text{s}^{-1}$, temperature change rate is about $2 \text{ }^\circ\text{C}/\text{min}$.

4. Result and discussion

4.1. Combined Tension-torsion Loading Experiment

Because of SMAs' unique properties, the experiments of uniaxial tension and torsion are necessary, and the tension-torsion simultaneous experiments are essential. The strain and stress curves of specimen $\text{Ni}_{47}\text{Ti}_{44}\text{Nb}_9$ experiments are shown in Fig.5, respectively, in $-20 \text{ }^\circ\text{C}$ and $-60 \text{ }^\circ\text{C}$. The pseudo-elasticity of SMAs is fully reflected. from the experiment results, we verified some special temperature ranges: the start temperature of the forward transformation before deformation is $M_s = -90 \text{ }^\circ\text{C} \pm 10 \text{ }^\circ\text{C}$, and the start temperature of the reverse transformation before deformation is $A_s = -65 \text{ }^\circ\text{C} \pm 10 \text{ }^\circ\text{C}$, and the finish temperature of the reverse transformation before deformation is $A_{f1} = -25 \text{ }^\circ\text{C} \pm 10 \text{ }^\circ\text{C}$.

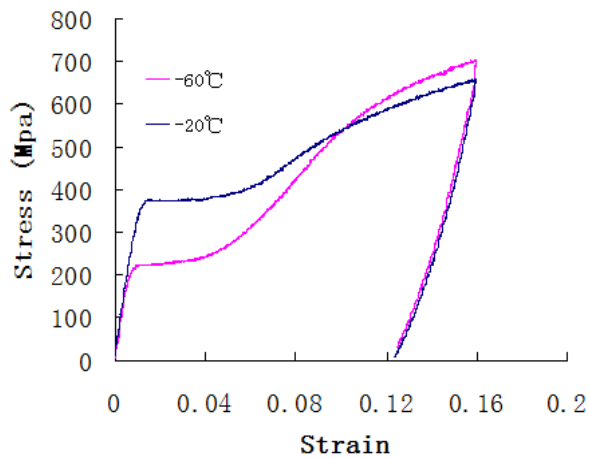


Figure 5. Combined tension-torsion loading experiment

4.2. Cooling Experiment

As we all know, SMAs are relatively sensitive to temperature, especially the temperature reduced gradually is essential to SMAs. However, the SMA experiments involving cooling are very seldom. Therefore, the special device was designed for SMA experiment research. Through the SMA specimen $\text{Ni}_{47}\text{Ti}_{44}\text{Nb}_9$ experimental results, we found that the strain curve of specimen $\text{Ni}_{47}\text{Ti}_4$ was gradually increased with the decrease of temperature as shown in Fig.6. Furthermore, through the specimen $\text{Ni}_{47}\text{Ti}_{44}\text{Nb}_9$ martensitic temperature $-20 \text{ }^\circ\text{C}$, we performed cyclic temperature loading on the specimen; the experimental results reflected the pseudo-elasticity. The start temperature of the forward transformation before deformation is $M_s = -90 \text{ }^\circ\text{C} \pm 10 \text{ }^\circ\text{C}$, and the start temperature of the reverse transformation before deformation is $A_s = -65 \text{ }^\circ\text{C} \pm 10 \text{ }^\circ\text{C}$, and the finish temperature of the reverse transformation before deformation is $A_{f1} = -25 \text{ }^\circ\text{C} \pm 10 \text{ }^\circ\text{C}$.

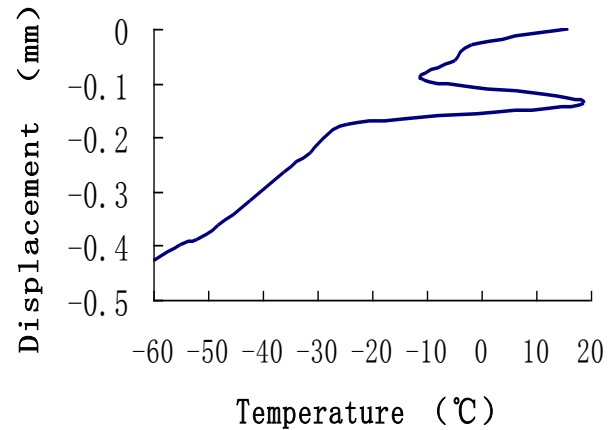


Figure 6. Cooling experiment

4.3. Low Temperature Experiment

SMAs are very sensitive to temperature changes, especially the low temperatures. From the last section, we know that the start temperature of the reverse transformation before deformation is $A_s = -65 \text{ }^\circ\text{C} \pm 10 \text{ }^\circ\text{C}$. In $-60 \text{ }^\circ\text{C}$, the strain and stress curves of specimen $\text{Ni}_{47}\text{Ti}_{44}\text{Nb}_9$ experiments, respectively, uniaxial tension experiment, torsion experiment and tension-torsion experiment are shown in Fig.7. The mechanical properties of SMAs are significantly different on the three kinds of loading methods. In the same strain of 16%, the stress of tension-torsion experiment is the lowest than the ones of uniaxial tension experiment and torsion experiment.

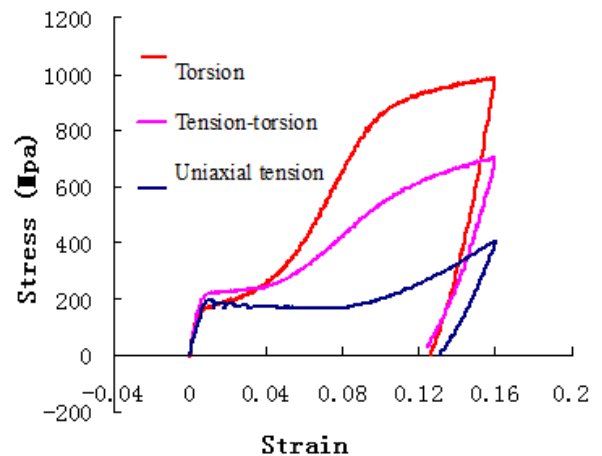


Figure 7. Experiments of different loading methods in $-60 \text{ }^\circ\text{C}$

4.4. Heating Experiment

From the last section, we know that SMAs are very sensitive to cooling progress. However, the performance of the cooling progress can not be used to predict the one of the heating progress, because of the unique composition and structure of SMAs. The heating experiment study must be carried out as shown in Fig.8. The torsion angle of specimen $\text{Ni}_{47}\text{Ti}_{44}\text{Nb}_9$ recovers slowly with the increase of experiment temperature, yet the angle recovers sharply in the start temperature of the martensitic transformation $65 \text{ }^\circ\text{C}$. When

the end to martensitic temperature is 90 °C, The torsion angle of specimen recovers almost no longer with the increase of experiment temperature. Shape memory effect is fully reflected.

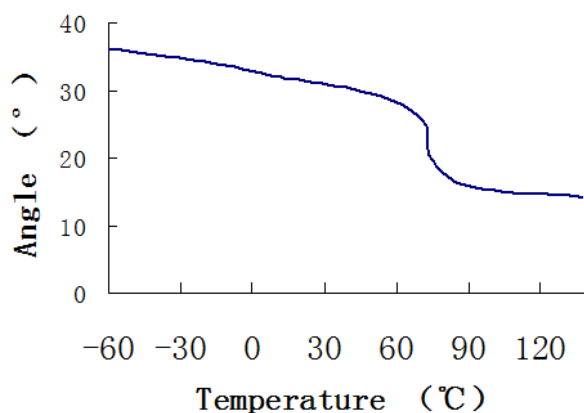


Figure 8. Heating experiment

When SMA specimen $Ni_{47}Ti_{44}Nb_9$ was subjected to tensile strain of 16%, the austenite transformation start temperature A_s and the austenite transformation finish temperature A_f could increase from -65 °C and -25 °C to, respectively, over 40 °C and around 70 °C. With this property, the deformed parts made of $Ni_{47}Ti_{44}Nb_9$ at low temperature can be stored at room temperature, instead of being stored at a low temperature, before assembled and recovered by heating, which is of significant importance for the application of this alloy in the practical application.

5. Conclusions

We introduced the special testing device of SMAs concerned with many factors and mainly include three parts, which were tension module, shearing module, and temperature-controlled cabinet, respectively. In work, it was assembled on MTS-858. The typical thermal-mechanical properties of SMAs were investigated systematically, involving the responses and the heating-induced strain recovery under proportional and non-proportional tensile-torsion loadings at various temperatures with SMA specimen $Ni_{47}Ti_{44}Nb_9$. There were main four kind experiments, including: combined tension-torsion loading experiments, cooling experiments, low temperature experiments and heating experiments. In addition, Recovery stress at various recovery strains and the thermal-mechanical properties of the alloy subjected to cyclic straining were investigated. We hope that this work can promote the further development of SMAs.

ACKNOWLEDGEMENTS

This work was financially supported by The National Natural Science Foundation of China (Grant No. 11702116), The National Natural Science Foundation of Jiangsu in

China (Grant No. BK20160484), and the Foundation of Jiangsu University (14JDG162).

REFERENCES

- [1] Zhou Miaolei, Wang Shoubin, Gao Wei. Hysteresis Modeling of Magnetic Shape Memory Alloy Actuator Based on Krasnosel'skii-Pokrovskii Model [J]. The Scientific World Journal. 2013. Article Number: 865176.
- [2] Achenbach M., Atanackovic T., Muller I. A model for memory alloys in plane strains [J]. Int. J. Solid. 1986.
- [3] Badami V., Ahuja B. Biosmart Materials: Breaking New Ground in Dentistry [J]. The Scientific World Journal. 2014. Article Number: 986912.
- [4] Abdul-Latif A., Chadli M. Modeling of the Heterogeneous Damage Evolution at the Granular Scale in Polycrystals Under Complex Cyclic Loadings [J]. International Journal of Damage Mechanics. 2007, Vol.16: P133-158.
- [5] Li Weiguo, Li Dingyu, Wang Ruzhuan, Fang Daining. Numerical Simulation for Thermal Shock Resistance of Thermal Protection Materials Considering Different Operating Environments [J]. The Scientific World Journal. 2013. Article Number: 324186.
- [6] Montalvao D., Francisca S., Braz F. Structural Characterisation and Mechanical FE Analysis of Conventional and M-Wire Ni-Ti Alloys Used in Endodontic Rotary Instruments [J]. The Scientific World Journal. 2014. Article Number: 976459.
- [7] Jin Huang, Xu Chen, Lirong Zhong. Analysis and Testing of MR Shear Transmission Driven by SMA Spring [J]. Advances in Materials Science and Engineering. 2013(2013), Article Number: 307207.
- [8] Hu Sun, Xianghe Peng, Kaiyuan Guo, Jingzhi Li, Jin Huang. Magnetorheological Materials Theory System and Experimental Investigation [J]. Materials Focus. 2013(4), Vol.2: P283-287.
- [9] Jianzuo Ma, Haolei Huang, Jin Huang. Characteristics Analysis and Testing of SMA Spring Actuator [J]. Advances in Materials Science and Engineering. 2013(2013), Article Number: 823594.
- [10] Tiger Sun, Xianghe Peng, Shuping Jiao, Changxing Xu, Jingzhi Li. Simulation of Particle Dynamics of Nano-Magnetorheological Materials in External Magnetic Fields [J]. Journal of Computational and Theoretical Nanoscience. 2014(6), Vol.11: P1518-1523.
- [11] Song Chen, Jin Huang, Hongyu Shu, Tiger Sun, Kailin Jian. Analysis and Testing of Chain Characteristics and Rheological Properties for Magnetorheological Fluid [J]. Advances in Materials Science and Engineering. 2013, Article Number: 290691.
- [12] Tiger Sun, Xianghe Peng, Jingzhi Li, Chao Feng. Testing Device and Experimental Investigation to Influencing Factors of Magnetorheological Fluid [J]. International Journal of Applied Electromagnetics and Mechanics. 2013(3), Vol.43: P283-292.

- [13] X. Peng, W. Pi, J. Fan. A microstructure-based constitutive model for the pseudoelastic behavior of NiTi SMAs [J]. *International Journal of Plasticity*. 2008(6), Vol.24: P 966–990.
- [14] B. Chen, X. Peng, X. Chen, J. Wang, H. Wang and N. Hu. A Three-Dimensional Model of Shape Memory Alloys under Coupled Transformation and Plastic Deformation [J]. *CMC-Computers Materials & Continua*. 2012(2), Vol.30: P 145-176.
- [15] Witos M. High Sensitive Methods for Health Monitoring of Compressor Blades and Fatigue Detection [J]. *The Scientific World Journal*. 2013. Article Number: 218460.
- [16] X. Peng, W. Pi, J. Fan. A Microstructure-Damage-Based Description for the Size Effect of the Constitutive Behavior of Pearlitic Steels [J]. *International Journal of Damage Mechanics*. 2010(7), Vol.19: P 821-849.
- [17] Ito W., Ito K., Umetsu R. Kinetic arrest of martensitic transformation in the NiCoMnIn metamagnetic shape memory alloy [J]. *Applied Physics Letters*. 2010(2), Vol.92. Article Number: 021908.